NASA TECHNICAL MEMORANDUM

NASA TM X-2806

NASA TM X-2806

PERFORMANCE COMPARISON OF A LOBED-DAISY MIXER NOZZLE WITH A CONVERGENT NOZZLE AT SUBSONIC SPEEDS

by Donald L. Maiden

Langley Research Center
Hampton, Va. 23665

NATIONAL AERONAUTICS AND SPACE ADMINISTRATION • WASHINGTON, D. C. • SEPTEMBER 1973

1. Report No.	2. Government Accession No.	3. Recipient's Catalog No.
NASA TM X-2806		

4. Title and Subtitle	5. Report Date
PERFORMANCE COMPARISON OF A LOBED-DAISY MIXER NOZZLE WITH A CONVERGENT NOZZLE AT SUBSONIC SPEEDS	September 1973
	6. Performing Organization Code
7. Author(s)	8. Performing Organization Report No.
Donald L. Maiden	L-8939
	10. Work Unit No.
9. Performing Organization Name and Address	501-24-06-01
NASA Langley Research Center Hampton, Va. 23665	11. Contract or Grant No.
	13. Type of Report and Period Covered
12. Sponsoring Agency Name and Address	Technical Memorandum
National Aeronautics and Space Administration Washington, D.C. 20546	14. Sponsoring Agency Code

15. Supplementary Notes

16. Abstract

An investigation to determine the performance, in terms of thrust minus nozzle axial force, of a lobed-daisy mixer nozzle has been conducted in the Langley 16-foot transonic tunnel at static conditions and at Mach numbers from 0.40 to 0.90 at angles of attack from -4° to 8°. Jet-total-pressure ratio was varied from about 1.2 to 2.0. The performance of a reference convergent nozzle with a similar nozzle throat area and length was used as a base line to evaluate the performance of the lobed-daisy mixer nozzle.

The results of this investigation indicate that with no external airflow (Mach number M of 0), and at values of jet-total-pressure ratio between 1.2 and 2.0, the static thrust exerted by the lobed-daisy mixer nozzle is less than that of the convergent nozzle by about 10 percent of ideal gross thrust. About 3.4 percent of the thrust loss was attributed to an unintentional internal area expansion in the fan passage. With external flow ($0.40 \leq M \leq 0.90$) the values of thrust minus nozzle axial force were much lower for the lobed-daisy mixer nozzle than for a reference convergent nozzle. At a jet-total-pressure ratio of 1.5 the performance difference between the two nozzles varied almost linearly from about 13 percent at $M = 0.40$ to about 20 percent at $M = 0.90$.

17. Key Word (Suggested by Author(s))	18. Distribution Statement
Noise-suppressor nozzle	Unclassified – Unlimited

19. Security Classif. (of this report)	20. Security Classif. (of this page)	21. No. of Pages	22. Price*
Unclassified	Unclassified	25	Domestic, $2.75 Foreign, $5.25

*For sale by the National Technical Information Service, Springfield, Virginia 22151

PERFORMANCE COMPARISON OF A LOBED-DAISY MIXER NOZZLE WITH A CONVERGENT NOZZLE AT SUBSONIC SPEEDS

By Donald L. Maiden
Langley Research Center

SUMMARY

An investigation to determine the performance, in terms of thrust minus nozzle axial force, of a lobed-daisy mixer nozzle has been conducted in the Langley 16-foot transonic tunnel at static conditions and at Mach numbers from 0.40 to 0.90 at angles of attack from -4^{o} to 8^{o}. Jet-total-pressure ratio was varied from about 1.2 to 2.0. The performance of a reference convergent nozzle with a similar nozzle throat area and length was used as a base line to evaluate the performance of the lobed-daisy mixer nozzle.

The results of this investigation indicate that with no external airflow (Mach number M of 0), and at values of jet-total-pressure ratio between 1.2 and 2.0, the static thrust exerted by the lobed-daisy mixer nozzle is less than that of the convergent nozzle by about 10 percent of ideal gross thrust. About 3.4 percent of the thrust loss was attributed to an unintentional internal area expansion in the fan passage. With external flow ($0.40 \leqq M \leqq 0.90$) the values of thrust minus nozzle axial force were much lower for the lobed-daisy mixer nozzle than for a reference convergent nozzle. At a jet-total-pressure ratio of 1.5 the performance difference between the two nozzles varied almost linearly from about 13 percent at $M = 0.40$ to about 20 percent at $M = 0.90$.

INTRODUCTION

In preparation for advanced short takeoff and landing (STOL) aircraft, the technology has included studies of turbofan powered-lift concepts with emphasis on externally blown flap (EBF) configurations. In the EBF concept bypass and primary exhausts (5-to-1 bypass ratio) are both directed against the wing flap system. The net result of this concept is a significant increase in the lift as well as, unfortunately, the perceived noise level. In order to meet the commonly considered goal for STOL aircraft of 95 EPNdB at 500 feet, the additional noise generated by the interaction of the jet exhaust with the flaps must be considerably reduced.

The flap interaction noise, according to references 1 and 2, appears to be proportional to the surface area of the flaps scrubbed by the jet exhaust and to the sixth power

of the jet-exhaust impingement velocity. Reducing this impingement velocity (while maintaining acceptable lift characteristics) appears to offer promise of substantial reduction in flap interaction noise.

The impingement velocity can be reduced by employing a mixer nozzle at the fan-jet engine exhaust. A mixer nozzle is a multielement nozzle designed in such a way that the velocity of the individual small jets making up the exhaust decays rapidly by turbulent mixing with the surrounding low velocity airstream. Unfortunately exhaust velocity is directly related to the thrust a nozzle can generate. Since the mixer nozzle will be used at all flight conditions, the nozzle must be designed to be as economically efficient as possible (i.e., to provide low specific fuel consumption through high thrust-minus-drag performance).

In order to evaluate the performance of a lobed-daisy type mixer nozzle, a wind-tunnel investigation has been conducted with the nozzle installed on an isolated nacelle in the Langley 16-foot transonic tunnel. The investigation was conducted in quiescent air and at Mach numbers from 0.40 to 0.90. The nozzle jet-total-pressure ratio was varied from about 1.2 to 2.0 and the angle of attack of the nacelle was varied from -4° to 8°.

SYMBOLS

A_b effective annular area between metal bellows and surrounding sleeves, m^2

A_e nozzle exit area, m^2

$A_{e,n}$ exhaust nozzle total exit area, in plane normal to axis, m^2

$A_{e,f}$ fan exhaust total exit area, m^2

$A_{l,f}$ local fan exhaust passage area, m^2

$A_{e,j}$ primary jet exhaust total exit area, m^2

$A_{l,j}$ local primary jet exhaust passage area, m^2

A_m model maximum cross-sectional area, m^2

A_t nozzle throat area, m^2

$A_{t,n}$ exhaust nozzle total throat area, m^2

$A_{t,f}$	fan exhaust throat area, m^2
D_f	external skin-friction drag of model between stations 52.07 cm and 121.92 cm, N
d_b	base diameter of convergent nozzle, cm
d_e	exit diameter of convergent nozzle, cm
d_m	model maximum diameter, 15.24 cm
$F_{A,n}$	nozzle external axial force (on portion aft of station 121.92 cm), positive downstream, N
F_{bal}	axial force indicated by balance, positive upstream, N
F_i	ideal isentropic gross thrust, N
F_j	gross thrust, positive upstream, N
l	nozzle length, cm
M	free-stream Mach number
$p_{b,d}$	pressure acting on downstream bellows, N/m^2
$p_{b,u}$	pressure acting on upstream bellows, N/m^2
p_{cav}	model internal cavity pressure, N/m^2
$p_{t,j}$	jet total pressure, N/m^2
p_∞	free-stream static pressure, N/m^2
R	circular-arc-boattail radius, cm
r	radial ordinate, normal to center line, cm
S	length of nozzle convergent section, cm

s	internal axial coordinate in convergent section, cm
t	nozzle throat length, cm
α	angle of attack, deg
β	nozzle terminal boattail angle, deg
β_c	nozzle chord boattail angle, deg
ϕ	radial angle of fan exhaust nozzle lobes, deg

APPARATUS AND METHODS

Wind Tunnel

The present investigation was conducted in the Langley 16-foot transonic tunnel, which is a single-return atmospheric wind tunnel with an octagonal slotted-throat test section and continuous air exchange. The tunnel has a continuously variable speed range from Mach 0.20 to 1.30.

Model and Support System

Shown in figure 1 is a photograph of the air-powered nacelle installed in the 16-foot transonic tunnel with a daisy-type mixer nozzle attached. Figure 2 presents a sketch of the single-engine simulator (with reference convergent nozzle) installed on the support system. The simulator was an air-powered cone-cylinder nacelle with a rounded shoulder at the junction of the conical nose and cylindrical section. In the simulator, dry high-pressure air at a stagnation temperature of about 274 K was introduced perpendicularly to the model axis into the portion supported by the balance shown by the fine section lines in figure 2. Air passage from the high-pressure plenum to the low-pressure plenum was through eight sonic nozzles equally spaced in angle around the axis of the high-pressure plenum. Since the high-pressure air was introduced radially to the model axis and an opposing nozzle cancels each nozzle thrust, the net axial force is zero. Therefore the balance measured only the gross thrust developed by the rearward acceleration of the air.

The low-pressure air chamber into which the air was introduced was sealed by a set of flexible metal bellows arranged so that the axial forces caused by pressurization of the system are compensating. The flow-smoothing screens in the model tail pipe were constructed of 0.635-mesh 0.0635-cm-diameter wire screen supported by four vanes. Aft

of the flow-smoothing screens an instrumentation section containing total temperature and total pressure probes is terminated at the nozzle connect location at model station 111.76 cm (see fig. 2).

The model was supported in the tunnel by a sting-strut support system; the nose of the model attached to the strut is shown in figures 1 and 2. The center line of the model was located on the wind-tunnel center line, with the center line of the sting which supports the strut 55.88 cm below that level. The sting portion of the system was 5.08 cm by 10.16 cm in cross section with the top and bottom capped by half-cylinders of 2.54-cm radius. The strut blade was 5 percent thick with a 50.8-cm chord in the streamwise direction. The strut-blade leading and trailing edges were swept 45°. Boundary-layer transition on the model was fixed by a 0.254-cm strip of No. 100 grit, 2.54 cm from the nose in accordance with techniques described in references 3 and 4.

Nozzle Configurations

Because of the similarity in nozzle areas and lengths (see fig. 3) the reference convergent nozzle shown in figures 2 and 4 was selected as a base line to evaluate the performance of the lobed-daisy mixer nozzle shown in figures 5 and 6. The reference convergent nozzle was constructed of aluminum to the geometric dimensions shown in figure 4. The unusual geometry of the lobed-daisy mixer nozzle is shown in figure 5. The forward-outside daisy lobes represent the fan exhaust nozzle and the aft-inside daisy lobes represent the primary jet exhaust nozzle.

Since both the fan exhaust and primary jet exhaust of the full-scale nozzle will operate at the same jet-total-pressure ratio $p_{t,j}/p_{\infty}$ the test-model nozzle required only a single air supply (see fig. 6). The lobed-daisy mixer nozzle was constructed of fiberglass and was designed to allow rotation of the primary jet exhaust nozzles. Two angular locations of the primary jet exhaust nozzles were investigated: one representing an in-line lobe configuration; and the other an interdigitated configuration as shown in figure 6.

The lobed-daisy mixer nozzle was originally designed as a convergent nozzle $\left(\text{i.e., } A_e/A_t = 1.0\right)$. Because of a catastrophic failure of the fiberglass nozzle (see fig. 7) at a jet-total-pressure ratio of about 1.8, reinforcing fiberglass had to be added to the wedge separating the fan passage lobes. The additional fiberglass changed the area distribution of the internal passage of the fan exhaust from converging to converging-diverging (see fig. 6). No change was made to the primary-jet-passage area distribution as a result of reinforcing the fiberglass nozzle. These effects on nozzle design are discussed in the section entitled "Results and Discussion."

Instrumentation

Data obtained during the investigation were recorded simultaneously on magnetic tape and were reduced to coefficient form by use of a computer. Approximately eight frames of data were taken over a time period of 8 seconds for each data point and the average value was used for computations.

A five-component strain-gage balance was used to measure forces and moments on that portion of the model downstream of the small gap at model station 52.07 cm (see fig. 2). Individual pressure transducers were used to determine jet total pressure and tare pressures (such as internal-cavity and bellows pressures). A total of 5 jet total pressures, 12 internal cavity pressures, and 2 bellows pressures were measured during the test. A thermocouple was used to measure jet total temperature. An electronic turbine flowmeter was used to determine the mass flow of the jet simulation air. The strut angle of attack was measured by a calibrated electrical potentiometer.

Data Reduction

The wind-tunnel data recorded on magnetic tape were used to compute standard force and pressure coefficients. All force and moment data in this report are referenced to the body axes through the center line of the jet simulator with the moment center located at model station 74.649 cm. The model angle of attack has been corrected for tunnel-flow angularity; however, no correction was made for deflection of the model support due to aerodynamic loading since this was known to be small.

The performance parameter used for presentation of results is thrust ratio; the thrust ratio is the ratio of actual jet thrust minus nozzle axial force to ideal jet thrust $\frac{F_j - F_{A,n}}{F_i}$ where

$$\left(F_j - F_{A,n}\right) = F_{bal} + \left(p_{cav} - p_\infty\right)A_m + \left(p_{b,d} - p_{b,u}\right)A_b + D_f$$

In the foregoing expression, the term F_{bal} is the axial force indicated by the balance, corrected for weight tares and balance interactions. The term $\left(p_{cav} - p_\infty\right)A_m$ is a tare-force correction for a pressure difference between the inside and outside of the model. The cavity pressure was measured at 12 locations within the model and each pressure was assumed to act on weighted area elements to which the sum equaled A_m, the maximum cross-sectional area. The term $\left(p_{b,d} - p_{b,u}\right)A_b$ is a bellows tare correction, which by design should be essentially zero. However, when internal flow velocities are large, a small pressure difference between the ends of the bellows can exist. In the present investigation the maximum bellows tare correction was less than one-half percent of ideal thrust. The term D_f is calculated flat-plate skin friction on the cylindrical portion of the afterbody between the gap at the metric break and the nozzle connect station.

For static tests, $M = 0$, the nozzle drag is zero and the thrust ratio reduces to F_j/F_i.

Tests

Tests were conducted in the Langley 16-foot transonic tunnel statically and at Mach numbers from 0.40 to 0.90 with the angle of attack varied from about -4^o to 8^o. The jet-total-pressure ratio $p_{t,j}/p_\infty$ was varied from jet off (1.0) to approximately 2.0. Reynolds number based on the maximum nacelle diameter of 15.24 cm (6.0 in.) varied from about 1.2×10^6 at $M = 0.40$ to 2.0×10^6 at $M = 0.90$.

RESULTS AND DISCUSSION

Static Performance

A comparison of the static-thrust ratios F_j/F_i of the reference convergent nozzle and the lobed-daisy mixer nozzle configurations is shown in figure 8. Generally, the static performance of the lobed-daisy nozzles was about 10 percent of ideal gross thrust $(0.1F_i)$ below that of the reference convergent nozzle over the range of jet-total-pressure ratio $p_{t,j}/p_\infty$ from about 1.2 to 2.0. The large thrust loss encountered with the lobed-daisy nozzles is attributed to increased friction losses due to an increase in internal wetted area and the area distribution of the internal fan exhaust passage (see fig. 6). As shown in figure 6 the fan passage has a minimum area, or throat area, which occurs about 6.6 cm (2.6 in.) forward of the fan exit area. The ratio of exit area to throat area for the fan passage is about 1.19, which represents a converging-diverging nozzle with a design pressure ratio of about 3.7. Since the area of the fan exhaust throat represents about 70 percent of the total nozzle sonic throat area, it is to be expected that the lobed-daisy nozzles will have higher thrust losses than the reference convergent nozzle operating near its lower design pressure ratio of 1.89. A theoretical analysis based on one-dimensional flow was made to estimate the thrust loss attributed to the converging-diverging area distribution of the fan passage. At $p_{t,j}/p_\infty = 2.0$ the overexpansion and divergence losses were calculated. These losses indicate that the test lobed-daisy nozzle internal performance F_j/F_i is about 3.4 percent lower than it would be if the fan-passage area distribution were converging. Therefore the performance of the lobed-daisy nozzle designed as a convergent nozzle should have an internal performance F_j/F_i of about 94.4 percent at a jet-total-pressure ratio of 2.0. The corrected internal performance of 94.4 percent agrees with the internal performance of similar noise suppressor nozzles with $A_{e,n}/A_m = 0.36$. An area distribution for the fan exhaust passage similar to the one shown for the primary jet passage in figure 6 would have increased the performance of the lobed-daisy mixer nozzle.

External-Flow Performance

The variation of $\frac{F_j - F_{A,n}}{F_i}$ with $p_{t,j}/p_\infty$ at $\alpha = 0^o$ is presented in figure 9. At all conditions much lower values of $\frac{F_j - F_{A,n}}{F_i}$ were obtained with the lobed-daisy mixer nozzle than with the reference convergent nozzle. A small improvement in performance with increasing $p_{t,j}/p_\infty$ is noted for the lobed-daisy mixer nozzle, which is probably a result of the slight increase in internal performance F_j/F_i with $p_{t,j}/p_\infty$ since the fan exhaust nozzle operates more efficiently near $p_{t,j}/p_\infty = 3.7$. Changing the location of the primary jet exhaust nozzles from in-line to interdigitated with the fan exhaust nozzles had little effect on the performance of the mixer nozzle at all test conditions.

The variation of $\frac{F_j - F_{A,n}}{F_i}$ with M at $p_{t,j}/p_\infty$ of 1.5 and 2.0 is shown in figure 10. At the selected jet-total-pressure ratios the lobed-daisy mixer nozzles become less efficient $\left(\text{i.e., lower } \frac{F_j - F_{A,n}}{F_i}\right)$ with increased Mach number. This loss in performance is probably because of an increase in nozzle drag with increased Mach number for the lobed-daisy mixer nozzle configurations. As noted earlier, the loss in performance is less at the higher jet-total-pressure ratio of 2.0 because of the slight increase in internal performance as $p_{t,j}/p_\infty$ approaches a value of 3.7. However, at $p_{t,j}/p_\infty = 1.5$ the difference in thrust minus nozzle axial force between the lobed-daisy mixer nozzle and the reference convergent nozzle increases almost linearly from about 13 percent at $M = 0.40$ to about 20 percent of ideal gross thrust at $M = 0.90$. At a higher jet-total-pressure ratio of 2.0 the difference is less, from about 11 percent at $M = 0.40$ to 16 percent at $M = 0.90$.

The variation of $\frac{F_j - F_{A,n}}{F_i}$ with $p_{t,j}/p_\infty$ at several values of angle of attack other than 0^o is presented in figure 11. These data were cross plotted in figure 12 to show the effect of angle of attack on $\frac{F_j - F_{A,n}}{F_i}$ at $p_{t,j}/p_\infty$ of 1.5 and 2.0. At both jet-total-pressure ratios, $\frac{F_j - F_{A,n}}{F_i}$ is shown to slightly decrease as the angle of attack is changed from 0^o. However, the effect of angle of attack on $\frac{F_j - F_{A,n}}{F_i}$ is small for small angles of attack ($\alpha < \pm 5^o$).

CONCLUSIONS

A wind-tunnel investigation to determine the performance of a lobed-daisy mixer nozzle with external flow has led to the following conclusions:

1. The static take-off thrust of the lobed-daisy nozzle configurations was about 10 percent of ideal gross thrust less than that obtained with the reference convergent nozzle. About 3.4 percent of the thrust loss was attributed to an unintentional internal area expansion in the fan exit passage.

2. At subsonic speeds the ratio of thrust minus nozzle axial force of the lobed-daisy mixer nozzle was significantly lower than that of the reference convergent nozzle. At a jet-total-pressure ratio of 1.5 the difference in thrust minus nozzle axial force for the two nozzles varied almost linearly from 13 percent of ideal gross thrust at a Mach number of 0.40 to 20 percent at a Mach number of 0.90.

3. Changing the location of the primary jet exhaust nozzles from in-line to interdigitated with the fan exhaust nozzles had little effect on the performance of the lobed-daisy mixer nozzle at all test conditions.

4. Small changes in angle of attack (less than $\pm 5^{o}$) had little effect on the performance of the lobed-daisy mixer nozzle.

Langley Research Center,
National Aeronautics and Space Administration,
Hampton, Va., June 25, 1973.

REFERENCES

1. Goodykoontz, Jack H.; Olsen, William A.; and Dorsch, Robert G.: Preliminary Tests of the Mixer Nozzle Concept for Reducing Blown Flap Noise. NASA TM X-67938, [1971].

2. Groesbeck, D.; Huff, R.; and Von Glahn, U.: Peak Axial-Velocity Decay With Mixer-Type Exhaust Nozzles. NASA TM X-67934, 1971.

3. Braslow, Albert L.; and Knox, Eugene C.: Simplified Method for Determination of Critical Height of Distributed Roughness Particles for Boundary-Layer Transition at Mach Numbers From 0 to 5. NACA TN 4363, 1958.

4. Braslow, Albert L.; Hicks, Raymond M.; and Harris, Roy V., Jr.: Use of Grit-Type Boundary-Layer-Transition Trips on Wind-Tunnel Models. NASA TN D-3579, 1966.

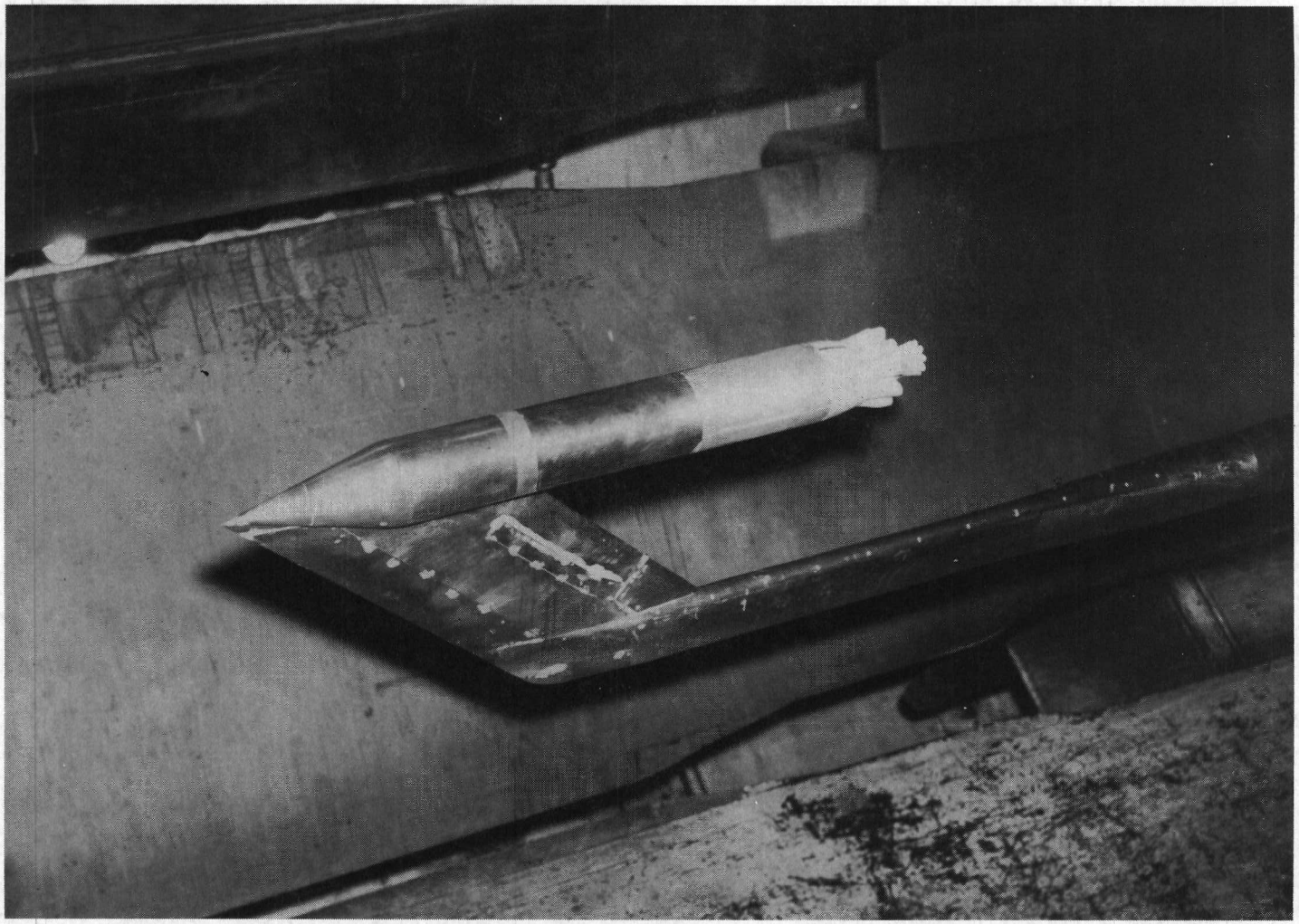

L-72-3549

Figure 1.- Air-powered nacelle mounted in the Langley 16-foot transonic tunnel with lobed-daisy mixer nozzle installed.

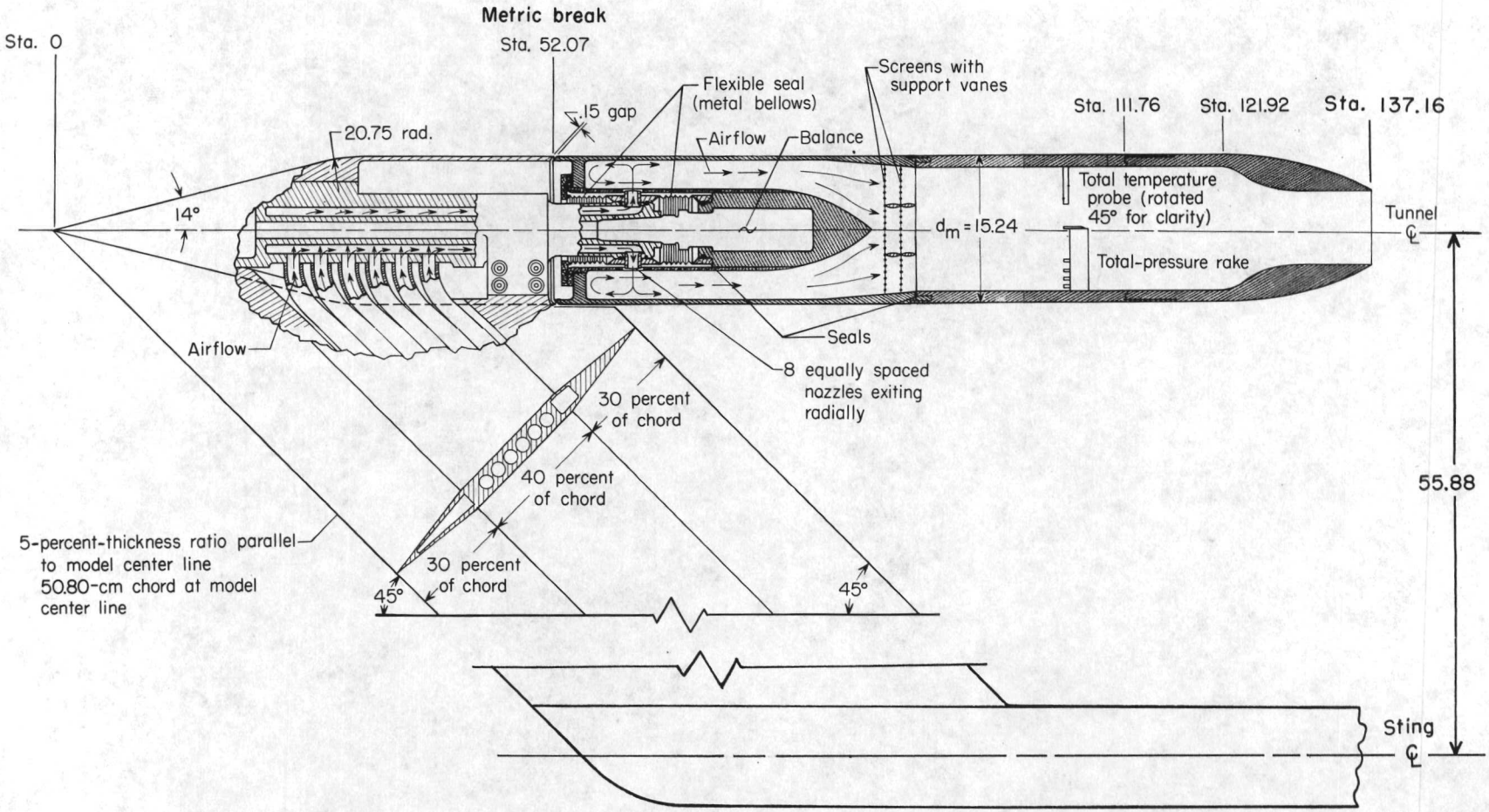

Figure 2.- Single-engine simulator showing installation of reference convergent nozzle.

L-73-3096

Figure 3.- Lobed-daisy mixer nozzle and reference convergent nozzle.

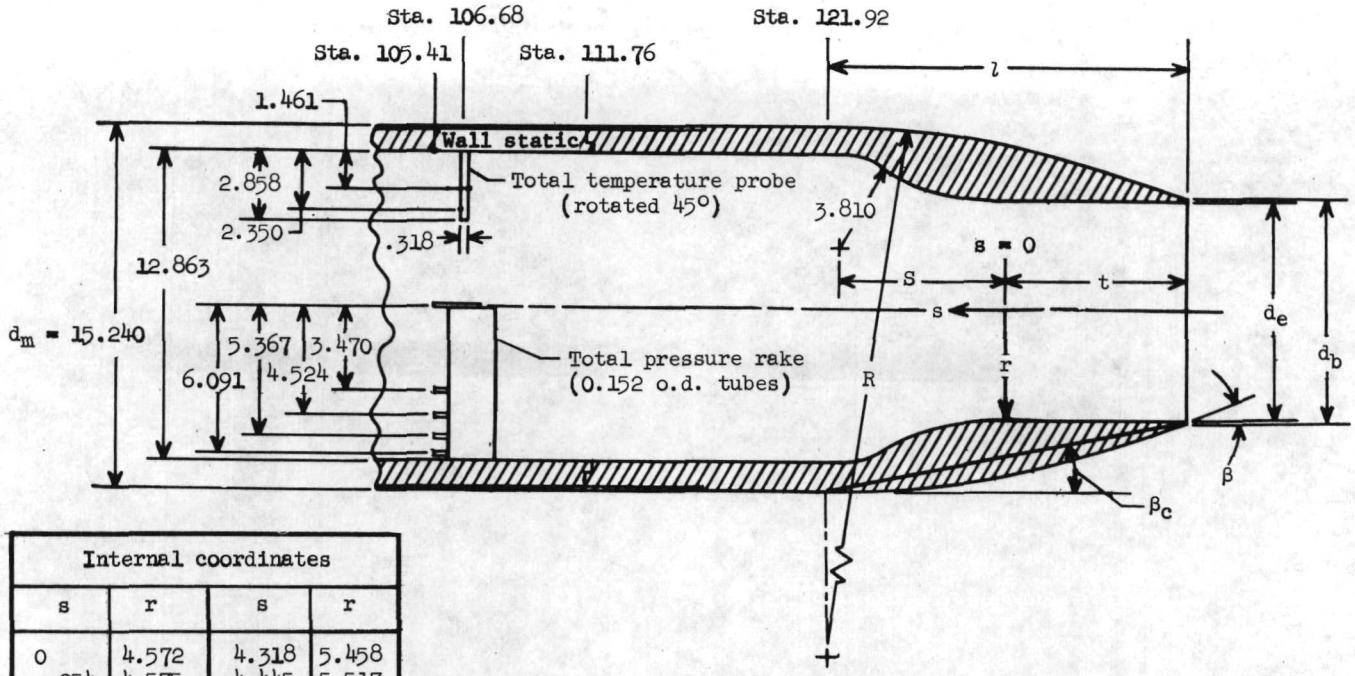

Internal coordinates			
s	r	s	r
0	4.572	4.318	5.458
.254	4.575	4.445	5.517
.508	4.582	4.572	5.578
.762	4.597	4.699	5.644
1.016	4.618	4.826	5.710
1.270	4.643	4.953	5.781
1.524	4.674	5.080	5.852
1.778	4.712	5.207	5.931
2.032	4.755	5.334	6.010
2.286	4.803	5.461	6.096
2.540	4.859	5.588	6.182
2.794	4.923	5.715	6.276
3.048	4.991	5.842	6.373
3.302	5.070	5.969	6.477
3.556	5.154	6.096	6.584
3.810	5.245	6.223	6.701
3.937	5.296	6.350	6.822
4.064	5.347	6.431	
4.191	5.403		

Geometric parameters							
l/d_m	d_e/d_m	d_b/d_m	R/d_m	t/d_m	S/d_m	β, deg	$β_c$, deg
1.00	0.60	0.61	2.662	0.500	0.462	22.07	11.03

Figure 4.- Detailed sketch of reference convergent nozzle with tables of geometric parameters and internal coordinates. All dimensions are in centimeters unless otherwise noted.

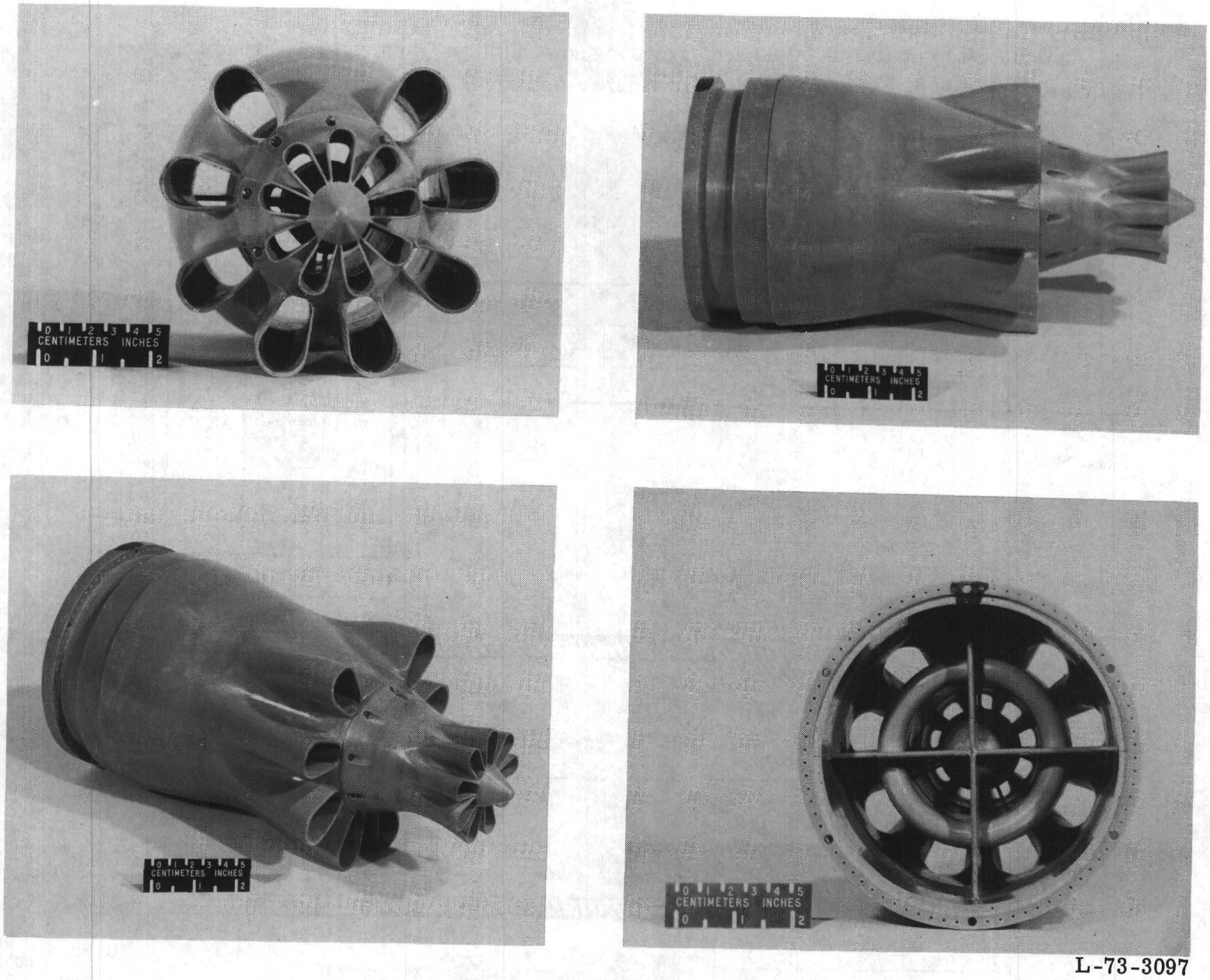

L-73-3097

Figure 5.- Geometry of lobed-daisy mixer nozzle.

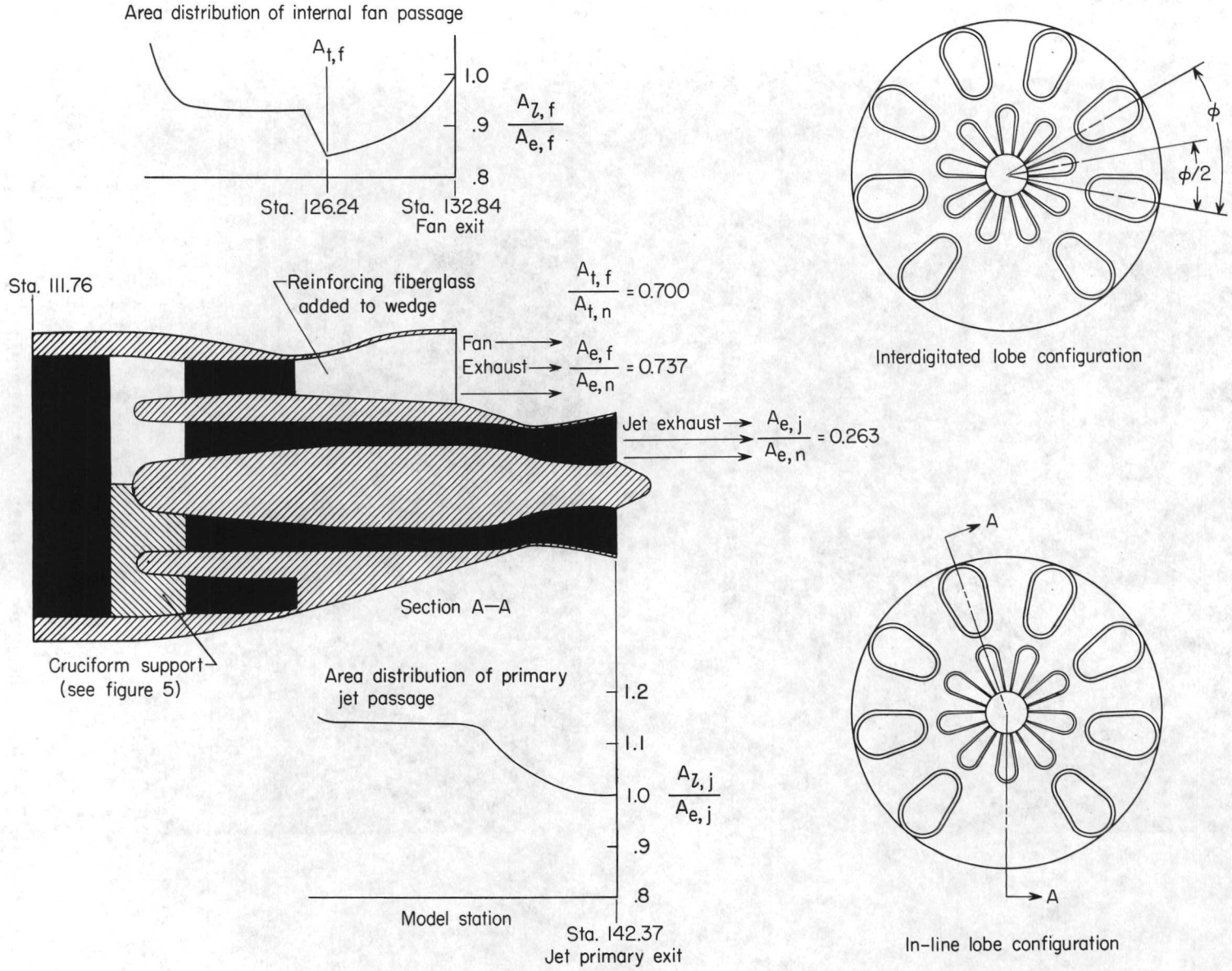

Figure 6.- Sketch of lobed-daisy mixer nozzle. All dimensions are in centimeters.

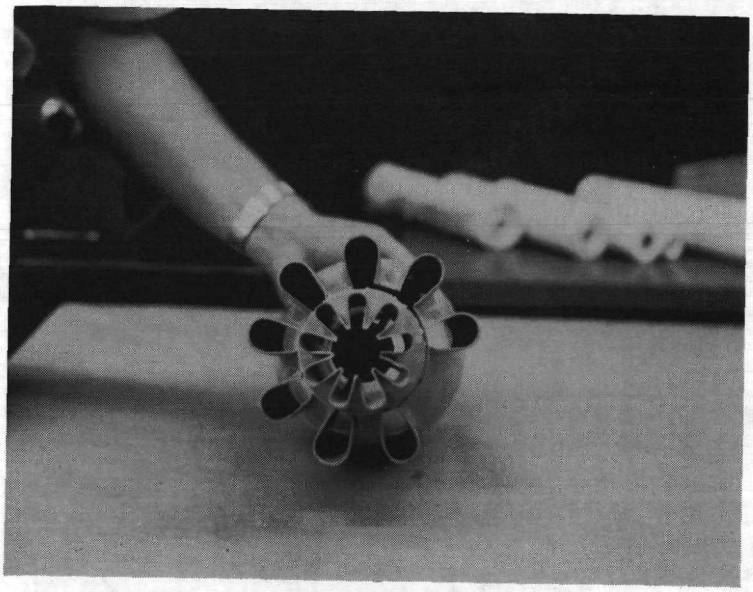

(a) Separation of fan exhaust lobes from nozzle boattail.

L-73-3098

(b) Separated terminal plug.

Figure 7.- Lobed-daisy mixer nozzle after catastrophic failure under pressurization.

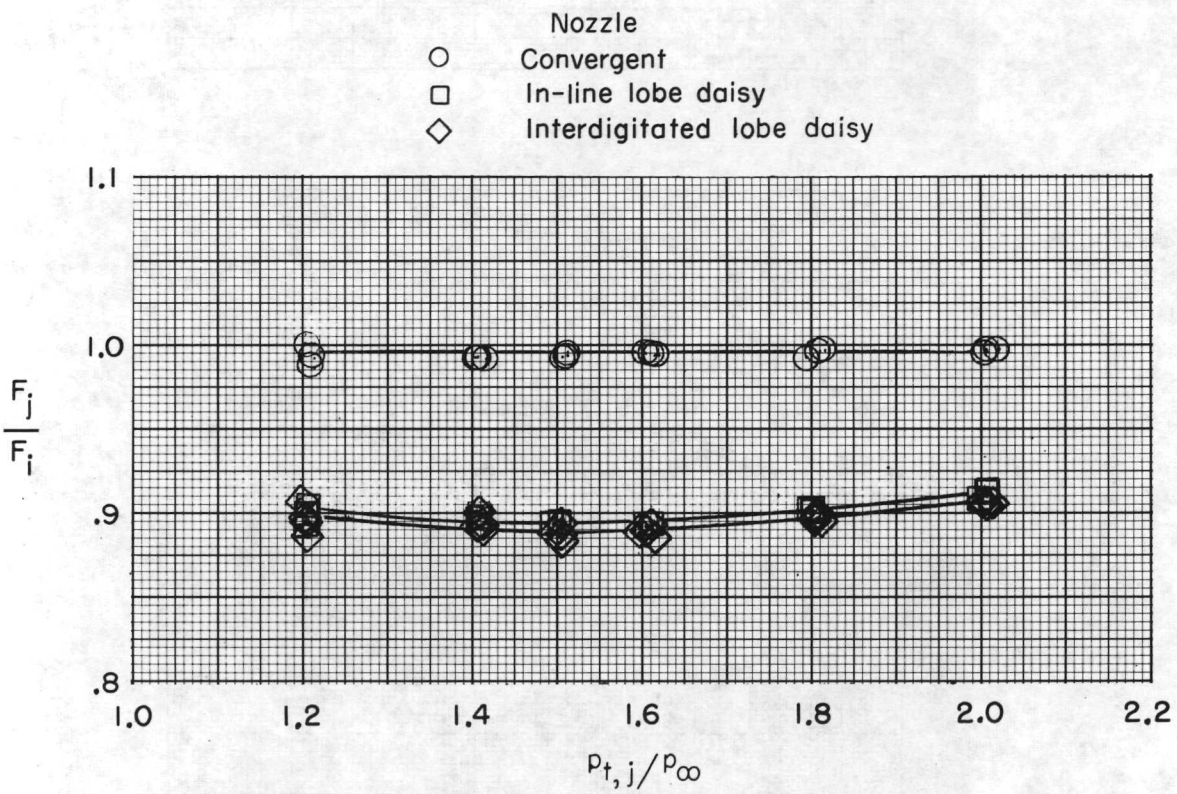

Figure 8.- Comparison of static-thrust ratios of lobed-daisy mixer nozzles and reference convergent nozzle.

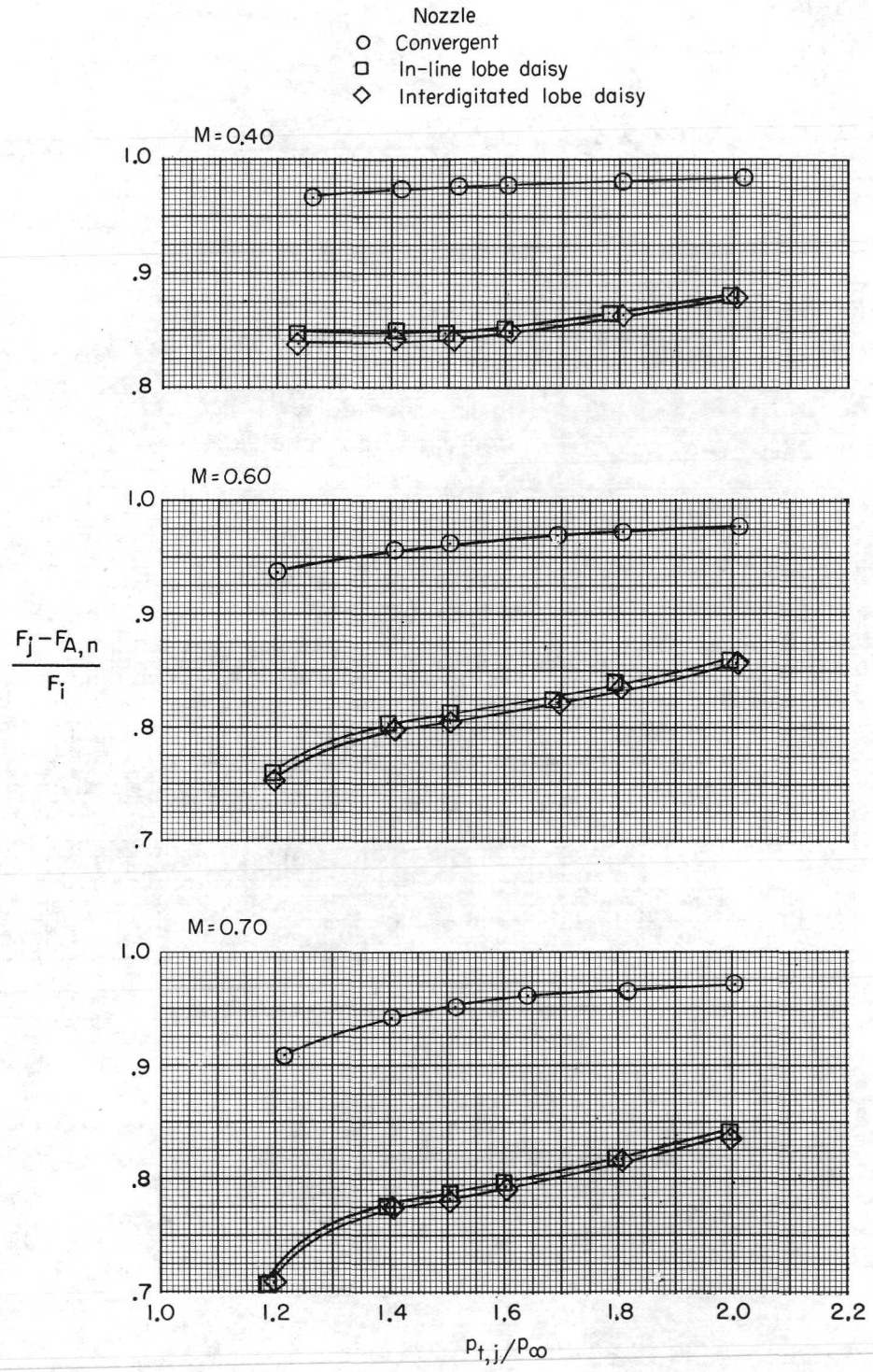

(a) M = 0.40, 0.60, and 0.70.

Figure 9.- Variation of $\frac{F_j - F_{A,n}}{F_i}$ with $p_{t,j}/p_\infty$ at $\alpha = 0^o$.

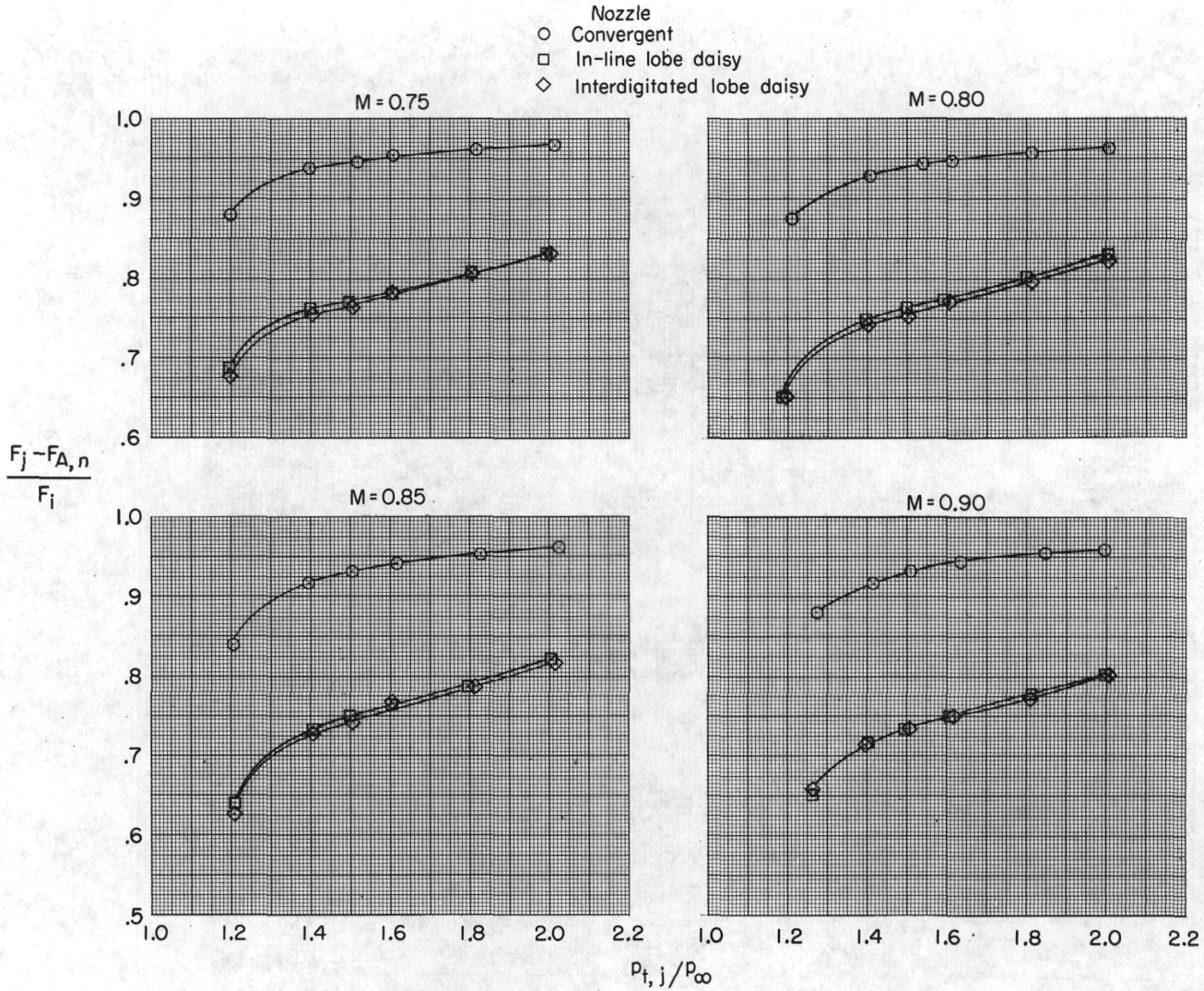

(b) M = 0.75, 0.80, 0.85, and 0.90.

Figure 9.- Concluded.

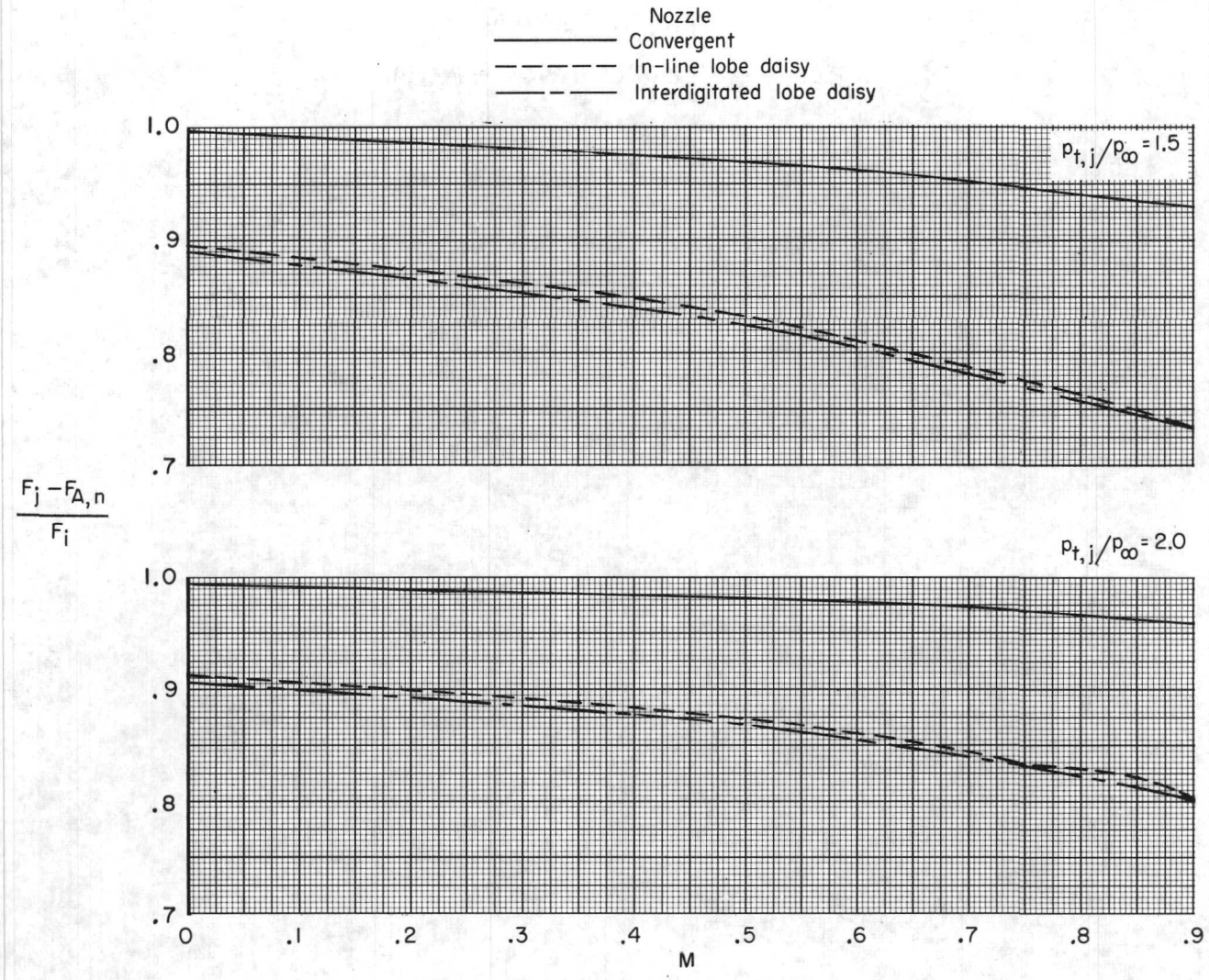

Figure 10.- Variation of $\frac{F_j - F_{A,n}}{F_i}$ with M at two jet-total-pressure ratios. $\alpha = 0^o$.

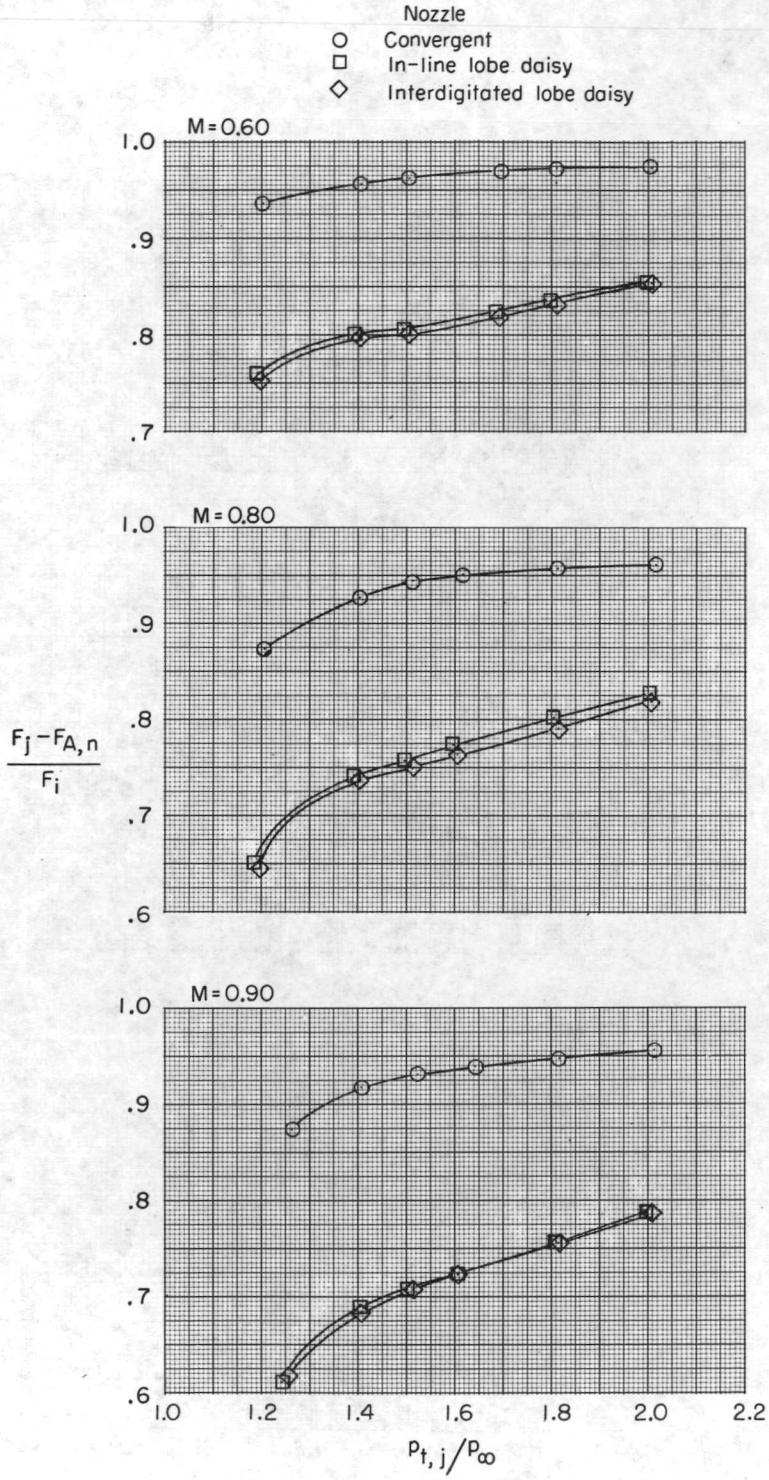

(a) $\alpha = -4^o$.

Figure 11.- Variation of $\frac{F_j - F_{A,n}}{F_i}$ with $p_{t,j}/p_\infty$ at several values of angle of attack.

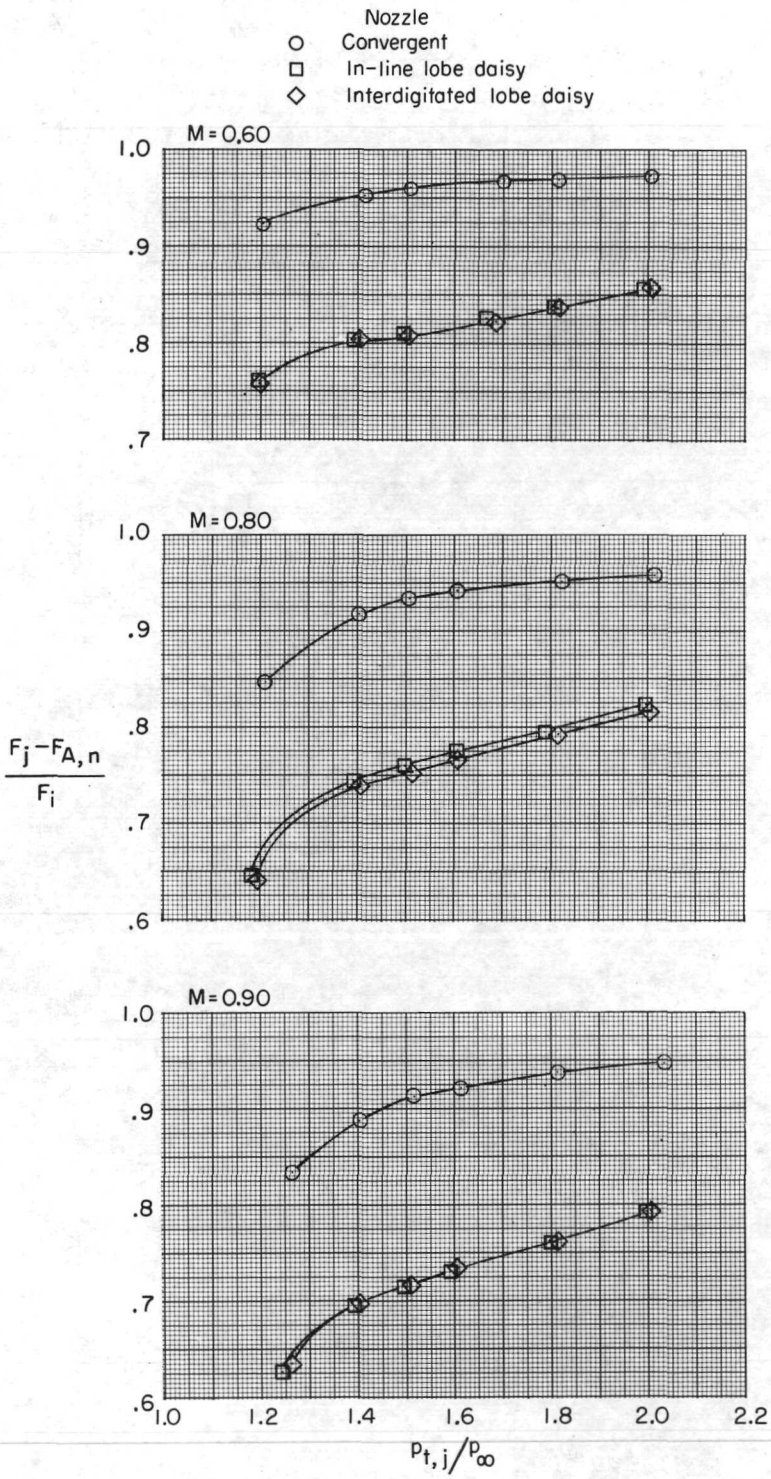

(b) $\alpha = 4^o$.

Figure 11.- Continued.

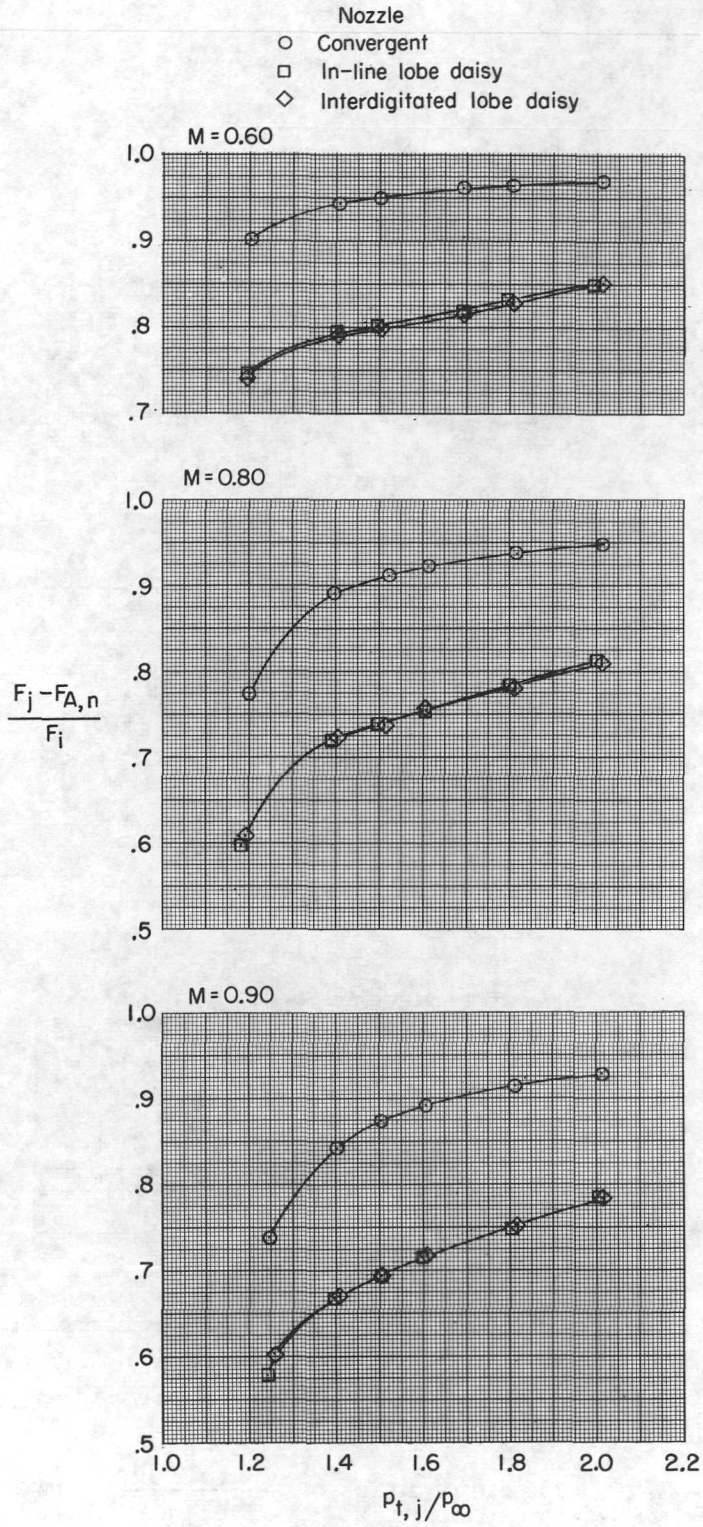

(c) $\alpha = 8^{\circ}$.

Figure 11.- Concluded.

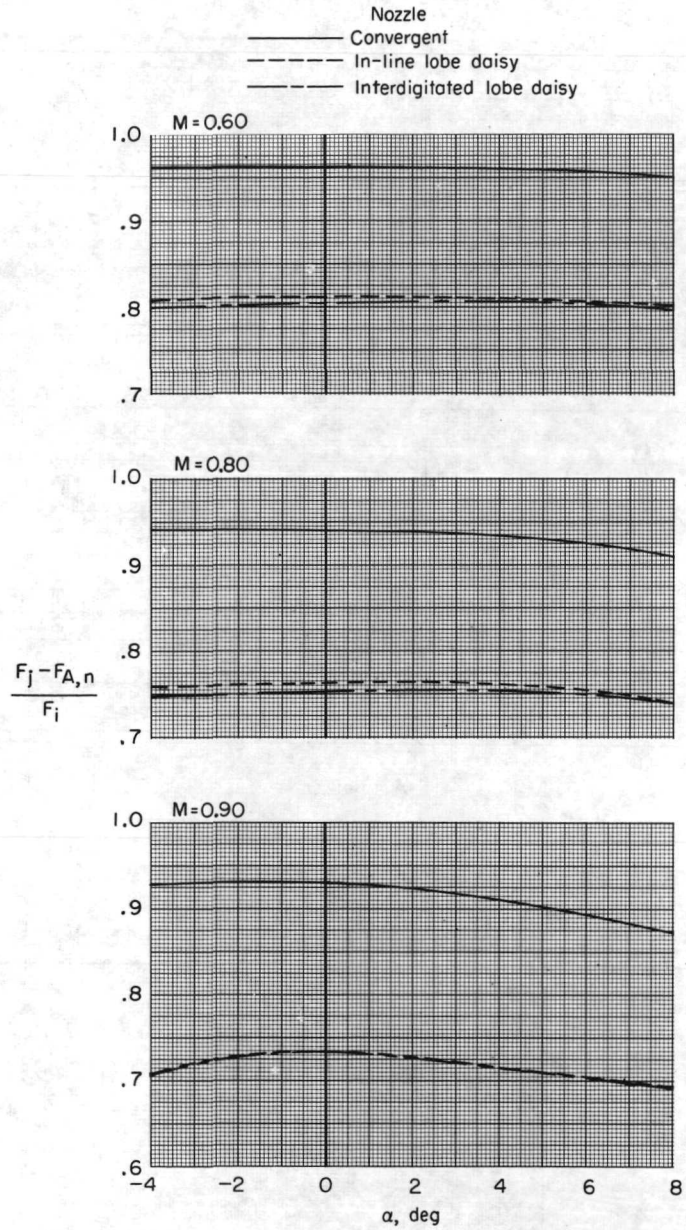

(a) $p_{t,j}/p_\infty = 1.5$.

Figure 12.- Effect of angle of attack on $\frac{F_j - F_{A,n}}{F_i}$ at two values of jet-total-pressure ratio.

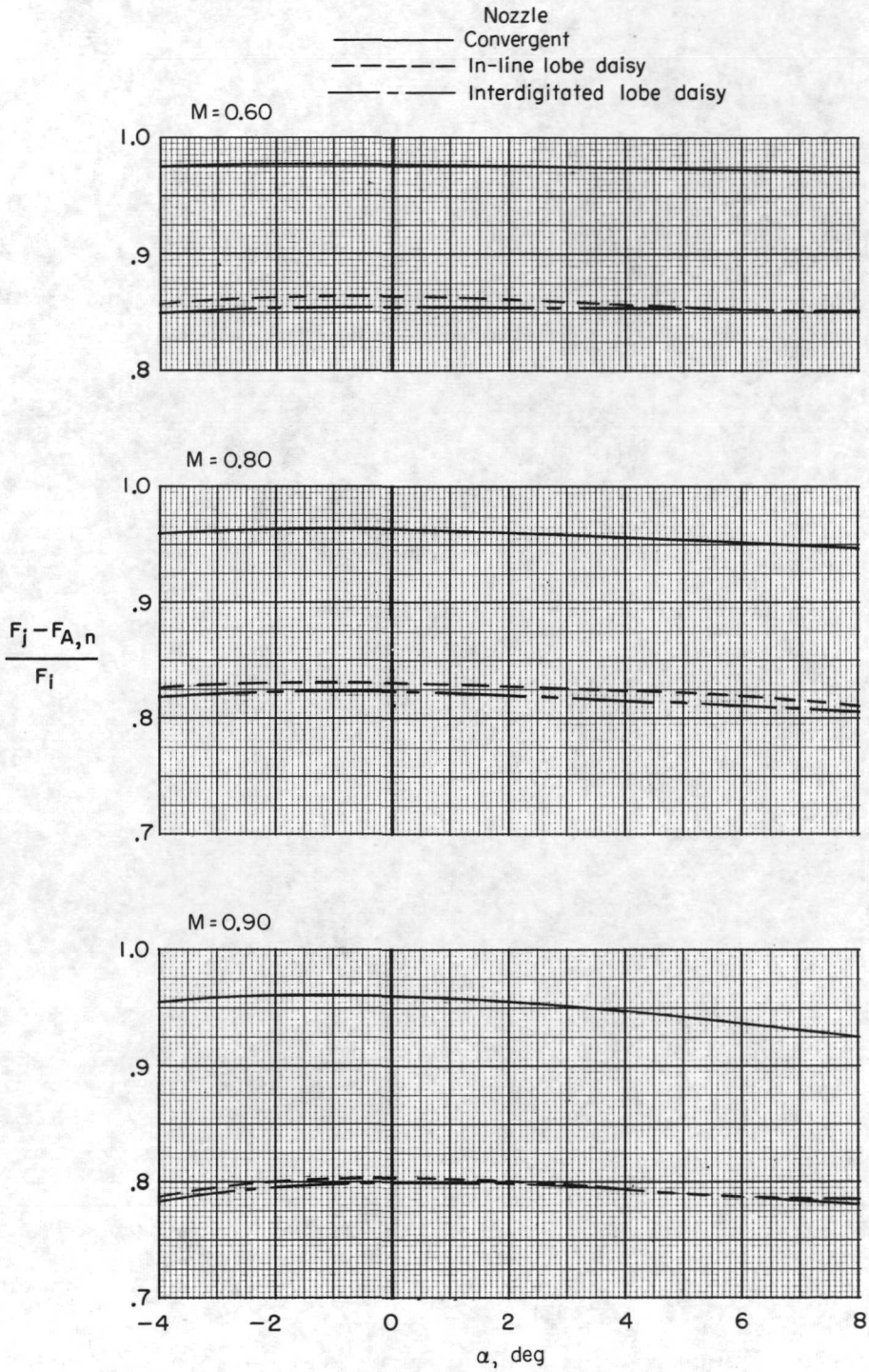

(b) $p_{t,j}/p_\infty = 2.0$.

Figure 12.- Concluded.

Page Intentionally Left Blank

NATIONAL AERONAUTICS AND SPACE ADMINISTRATION
WASHINGTON, D.C. 20546

OFFICIAL BUSINESS
PENALTY FOR PRIVATE USE $300

SPECIAL FOURTH-CLASS RATE
BOOK

POSTAGE AND FEES PAID
NATIONAL AERONAUTICS AND
SPACE ADMINISTRATION
451

U.S.MAIL

POSTMASTER: If Undeliverable (Section 158 Postal Manual) Do Not Return

"The aeronautical and space activities of the United States shall be conducted so as to contribute . . . to the expansion of human knowledge of phenomena in the atmosphere and space. The Administration shall provide for the widest practicable and appropriate dissemination of information concerning its activities and the results thereof."

—NATIONAL AERONAUTICS AND SPACE ACT OF 1958

NASA SCIENTIFIC AND TECHNICAL PUBLICATIONS

TECHNICAL REPORTS: Scientific and technical information considered important, complete, and a lasting contribution to existing knowledge.

TECHNICAL NOTES: Information less broad in scope but nevertheless of importance as a contribution to existing knowledge.

TECHNICAL MEMORANDUMS: Information receiving limited distribution because of preliminary data, security classification, or other reasons. Also includes conference proceedings with either limited or unlimited distribution.

CONTRACTOR REPORTS: Scientific and technical information generated under a NASA contract or grant and considered an important contribution to existing knowledge.

TECHNICAL TRANSLATIONS: Information published in a foreign language considered to merit NASA distribution in English.

SPECIAL PUBLICATIONS: Information derived from or of value to NASA activities. Publications include final reports of major projects, monographs, data compilations, handbooks, sourcebooks, and special bibliographies.

TECHNOLOGY UTILIZATION PUBLICATIONS: Information on technology used by NASA that may be of particular interest in commercial and other non-aerospace applications. Publications include Tech Briefs, Technology Utilization Reports and Technology Surveys.

Details on the availability of these publications may be obtained from:

SCIENTIFIC AND TECHNICAL INFORMATION OFFICE

NATIONAL AERONAUTICS AND SPACE ADMINISTRATION

Washington, D.C. 20546